J. Fluid Mech. (1972), *vol.* 51, *part* 3, *pp.* 529–543
Printed in Great Britain

Two-dimensional free-surface gravity flow past blunt bodies

By G. DAGAN

Technion, Israel Institute of Technology, Haifa and
Hydronautics Ltd, Rehovoth, Israel

AND M. P. TULIN

Hydronautics Inc., Laurel, Maryland

(Received 12 January 1970 and in revised form 22 September 1971)

Most of the wave resistance of blunt bow displacement ships is caused by the bow-breaking wave. A theoretical study of the phenomenon for the two-dimensional steady flow past a blunt body of semi-infinite length is presented. The exact equations of free-surface gravity flow are solved approximately by two perturbation expansions. The small Froude number solution, representing the flow beneath an unbroken free surface before the body, is carried out to second order. The breaking of the free surface is assumed to be related to a local Taylor instability, and the application of the stability criterion determines the value of the critical Froude number which characterizes breaking. The high Froude number solution is based on the model of a jet detaching from the bow and not returning to the flow field. The outer expansion of the equations yields the linearized gravity flow equations, which are solved by the Wiener–Hopf technique. The inner expansion gives a nonlinear gravity-free flow in the vicinity of the bow at zero order. The matching of the inner and outer expansions provides the jet thickness as well as the associated drag.

1. Introduction

The conventional linearized theory of ship waves is based on a first-order perturbation expansion in which the length Froude number Fr_L is of order one, while the beam Froude number (thin ships) and/or the draft Froude number Fr_T (slender or flat ships) tend to infinity. While the theory is in fair agreement with laboratory results in the case of schematical fine shapes (e.g. Weinblum, Kendrick & Todd 1952) it is of a qualitative value at best in the case of actual hulls. To improve the accuracy of the linearized solutions, second-order nonlinear effects have been considered either with the free-surface condition or with the body condition (e.g. Tuck 1965; Eggers 1966).

A different nonlinear effect, overlooked until recently for the case of displacement ships, is that associated with the bow bluntness. It is well known from the theory of inviscid flow past aerofoils or slender bodies (Van Dyke 1964) that the linearized solution is singular near a blunt nose in the stagnation region. The singularity may be removed by an inner expansion in which the length scale is

a local one associated with the nose bluntness. In the case of a free-surface flow with gravity the phenomenon is more complex. The pressure rise in the stagnation region is associated with the free-surface rise and, henceforth, with a change in the boundary of the flow domain.

Our analysis suggests the following picture of the change of the steady flow pattern near a blunt bow as the Froude number increases (figure 1). (i) At small Fr_T ($Fr_T = U'/(g/T')^{\frac{1}{2}}$ (where U' is the velocity at infinity, T' is the draft), see figure 1 (*a*), the free surface is smooth and stable, being horizontal at the stagnation point. The bow drag is zero in this range. (ii) At a certain critical Fr_T the free surface becomes unstable and breaks. We assume that the instability is of the type studied by Taylor (1950): in the region of convexity of the free surface the centrifugal acceleration (directed outwards) offsets the gravity acceleration when the critical condition is attained and locally the total normal acceleration vanishes. The Taylor local instability criterion may be also stated in terms of the pressure gradient: at Froude numbers larger than the critical one the pressure gradient normal to the free surface is negative, i.e. pressures smaller than the atmospheric prevail in the water body. (iii) At larger Fr_T a stable breaking wave (figure 1 (*b*)) develops in front of the bow. Owing to the energy loss in the breaking wave the free-surface rise near the body is smaller than the ideal rise and the body experiences a genuine drag force. (iv) At high Fr_T the rise of the bow-returning jet is relatively high and the flow becomes somehow similar to that encountered in planing problems. With the neglect of the returning jet, the bow drag becomes equal to the jet momentum loss.

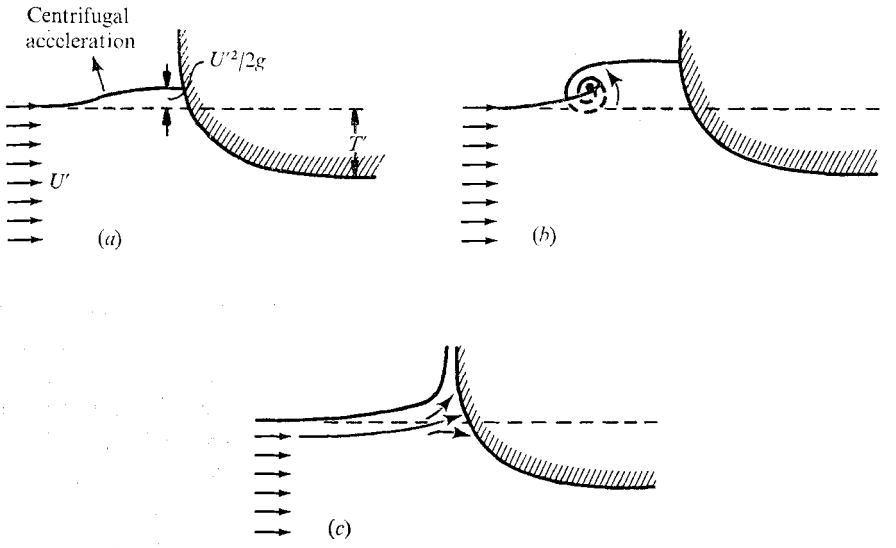

FIGURE 1. The changes in the flow regime associated with increasing Froude number Fr_T. (*a*) Smooth free surface, (*b*) breaking wave, (*c*) jet.

A systematic experimental confirmation of the role played by the bow bluntness of displacement ships has been provided recently by Baba (1969). From towing tank tests with three geosims of a tanker ($C_b = 0{\cdot}77$) it was found that in ballast conditions at $Fr_T \approx 1{\cdot}2$ a breaking wave appears before the bow. At the

maximum Fr_L tests ($Fr_L = U'/(gL')^{\frac{1}{2}} = 0{\cdot}24$, $Fr_T = 1{\cdot}7$) the energy dissipated in the breaking wave contributed 18 per cent of the total resistance, while the energy radiated by waves gave only 6 per cent. Baba has suggested a two-dimensional representation of the breaking wave of this experiment, as if it were uniform and normal to the bow, and has estimated its equivalent length as roughly half the beam. The drag coefficient per unit length, corresponding to a two-dimensional flow across the breaking wave is $C_D = D'/\frac{1}{2}\rho U'^2 T' = 0{\cdot}08$, where D' is the drag force, for $Fr_T = 1{\cdot}7$ (Baba 1969, § 7.3). With the development of large tankers, as well as large and rapid cargo ships, the study of the bow free-surface nonlinear effect therefore becomes particularly important.

We present here some studies and results which are reported in detail in two reports (Dagan & Tulin 1969, 1970). In some cases the present results correct and supplant the earlier work. In this first stage we have attacked the two-dimensional problem of steady free-surface flow of an inviscid liquid past a blunt body of semi-infinite length. The two-dimensional study is a necessary step in the development of a theory for three-dimensional bows since it provides a valuable gain in insight at the expense of relatively simple computations. Moreover, it gives an estimate of the bow drag of flat ships and opens the way to more realistic computations by further approximations.

Taking the length as semi-infinite is very useful from a mathematical point of view and it is equivalent to the limit $Fr_L \to 0$. This assumption is entirely justified for the small Fr_L considered here and for determination of the bow flow, which is not sensibly influenced by the trailing edge condition. We are assuming in fact that the location of the body beneath the unperturbed upstream level is determined entirely by the buoyancy, while the dynamical effects are localized at the edges. Here lies the main difference between the solution presented in the present work for high Fr_T and the solutions of the planing plate (Squire 1957) in which the body position is not assigned *a priori*.

The flow problem, even in the two-dimensional case, is still difficult because of the nonlinearity of the free-surface condition. For this reason we consider here two asymptotic expansions of the exact equations of steady flow in the only dimensionless parameter of the problem: Fr_T. The small Fr_T solution covers the regime of figure 1(*a*), including the derivation of the breaking condition. The second, high Fr_T, solution applies to the case shown in figure 1(*c*) and permits the computation of the bow drag. The intermediate case (figure 1(*b*)) is left for future studies.

2. The small Froude number solution

2.1. *Free-surface gravity flow near a stagnation point*

We consider first the exact solution for the angle between the free surface and a rigid boundary at a stagnation point (figure 2). In the symmetrical case ($\lambda_1 = \pi - \lambda_2$) the classical Stokes result (Wehausen & Laitone 1960) requires that $\lambda = \lambda_2 - \lambda_1 = \frac{2}{3}\pi$. This result will now be extended for other possible angles between AO and OB.

In the vicinity of O ($z = 0$, figure 2(a)) we assume that the z plane is mapped on the complex potential plane f (figure 2(b)) by

$$z = \alpha e^{-i\lambda_1} f^{\lambda/\pi} + R(f), \tag{1}$$

AOB obviously being a streamline, $f = f'g/U'^3$, f' being the complex potential. The constant α is real and positive so that AO is mapped on the positive ϕ axis.

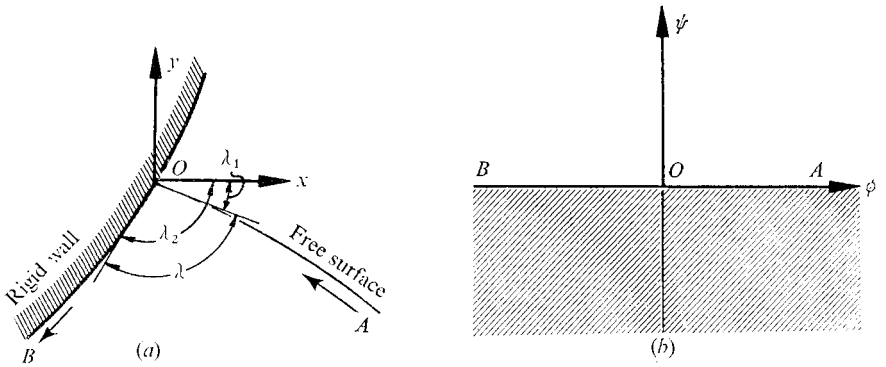

FIGURE 2. Free-surface flow in the vicinity of a stagnation point.
(a) Complex z plane, $z = x + iy$, (b) complex f plane, $f = \phi + i\psi$.

The function R, which has to vanish at O, is assumed to be of the form

$$R = \beta e^{i\sigma} f^{\gamma} \tag{2}$$

in the vicinity of O, with β, σ and γ real numbers. Obviously $\gamma > \lambda/\pi$, otherwise the mapping of the corner AOB is not ensured.

In order to apply the Bernoulli equation along AO let us determine y and $q^2 = u^2 + v^2$ as functions of ϕ. From (1) and (2) we obtain on AO ($f = \phi$)

$$y = -\alpha \sin \lambda_1 \phi^{\lambda/\pi} + \beta \sin \sigma \phi^{\gamma}, \tag{3}$$

$$x = \alpha \cos \lambda_1 \phi^{\lambda/\pi} + \beta \cos \sigma \phi^{\gamma}, \tag{4}$$

$$1/q^2 = x_{,\phi}^2 + y_{,\phi}^2 = (\alpha\lambda/\pi)^2 \phi^{2(\lambda/\pi - 1)} + 2(\alpha\beta\lambda\gamma/\pi) \cos(\lambda_1 + \sigma) \phi^{(\lambda/\pi + \gamma - 2)}. \tag{5}$$

By expanding (5) near $\phi = 0$, q^2 is found to be

$$q^2 = (\pi/\lambda\alpha)^2 \phi^{-2(\lambda/\pi - 1)} [1 - 2(\pi\beta\gamma/\alpha\lambda) \phi^{\gamma - \lambda/\pi} \cos(\lambda_1 + \sigma) + \ldots]. \tag{6}$$

Substituting y and q^2 into Bernoulli's equation and retaining terms of order $\phi^{(2-\lambda/\pi)}$ or ϕ^2 at most, we get

$$y + \frac{q^2}{2g} = -\alpha \sin \lambda_1 \phi^{\lambda/\pi} + \beta \sin \sigma \phi^{\gamma} + \frac{1}{2g} \left(\frac{\pi}{\lambda\alpha}\right)^2 \phi^{-2(\lambda/\pi - 1)} + \ldots \equiv 0. \tag{7}$$

The identity (7) yields the following relationships between λ_1 and λ: (i) If $\lambda_1 \neq 0$, the first and third terms of (7) give

$$\lambda = \tfrac{2}{3}\pi, \quad \frac{1}{2\alpha} \left(\frac{\pi}{\lambda\alpha}\right) = g \sin \lambda_1. \tag{8}$$

This is Stokes's classical result. Obviously $\lambda_2 \geqslant \frac{2}{3}\pi$, for otherwise $\alpha < 0$ and the free surface descends towards a stagnation point which is in contradiction with

the Bernoulli equation. (ii) If $\lambda_1 = 0$ the first term of (7) vanishes and the remaining terms give

$$\gamma = -2(\lambda/\pi - 1). \tag{9}$$

Since $\gamma > \lambda/\pi$ equation (9) shows that $\lambda < \frac{2}{3}\pi$. A particular case is that of $\gamma = 1$, which makes the function R analytic. In this case (9) gives $\lambda = \frac{1}{2}\pi$, i.e. the confluence between a horizontal free surface and a vertical wall.

In conclusion, there are two possible angles between a free surface and a rigid wall at the stagnation point: (i) If the wall is inclined with respect to the horizontal at an angle larger than $\frac{2}{3}\pi$ ($\frac{2}{3}\pi < \lambda_2 < \pi$) the free surface intersects the wall at $\frac{2}{3}\pi$ ($\lambda = \frac{2}{3}\pi$). (ii) If the wall is inclined at less that $\frac{2}{3}\pi$ ($\lambda < \frac{2}{3}\pi$) the free surface is horizontal ($\lambda_1 = 0$). In the latter case the equation of the free surface near the origin is

$$y = \beta \sin \sigma(x/a)^{2(\pi/\lambda - 1)} \tag{10}$$

and the curvature of the free surface becomes infinite for $\lambda > \frac{1}{2}\pi$ and $x \to 0$. The free surface is, however, stable since the dynamical part of the normal pressure gradient, given by

$$\partial p/\partial y = \rho(u^2/r) = \rho q^2 \, d^2y/dx^2,$$

vanishes since (6) and (10) show that

$$\partial p/\partial y \sim x^{2(2\pi/\lambda - 3)}. \tag{11}$$

Hence the pressure is hydrostatically distributed in the vicinity of the stagnation point.

2.2. *Small Fr_T perturbation expansion*

We consider the flow past a semi-infinite body (figure 3) and an expansion near the state of rest, for small Fr_T. Referring the variables to T' and $(gT')^{\frac{1}{2}}$ and expanding as follows:

$$F(Z) = \Phi + i\Psi = Fr_T F_1(Z) + Fr_T^2 F_2(Z) + Fr_T^5 F_3(Z) + \ldots, \tag{12}$$

$$W(Z) = U - iV = Fr_T W_1(Z) + Fr_T^3 W_2(Z) + Fr_T^5 W_3(Z) + \ldots, \tag{13}$$

$$N(X) = Fr_T^2 N_1(X) + Fr_T^4 N_2(X) + Fr_T^6 N_3(X) + \ldots, \tag{14}$$

where $F = f'/g^{\frac{1}{2}}T'^{\frac{3}{2}}$; $W = w'/(gT')^{\frac{1}{2}}$, w' being the complex velocity; $N = \eta'/T'$, η' being the free-surface elevation; $Z = zU'^2/gT'$. We thus obtain from the exact free-surface conditions (Bernoulli equation and the streamline condition) and the body boundary condition the following equations.

At first order (figure 3(*b*))

$$\Psi_1 = 0 \quad (ASBA), \tag{15}$$

$$W_1 = 1 \quad (X \to -\infty), \tag{16}$$

i.e. a flow beneath a rigid wall replacing the free surface at its unperturbed elevation. In addition

$$N_1 = \tfrac{1}{2}(1 - U_1^2) \quad (X < 0,\ Y = 0). \tag{17}$$

At second order

$$\Psi_2 = -U_1 N_1 \quad (AS, X < 0,\ Y = 0), \tag{18}$$

$$\Psi_2 = 0 \quad (SBA, X > 0,\ Y = H(X)), \tag{19}$$

$$N_2 = -U_1 U_2 \quad (X < 0,\ Y = 0); \tag{20}$$

at third order

$$\Psi_3 = -(U_1 N_2 + U_2 N_1) \quad (AS, X < 0, Y = 0), \tag{21}$$

$$\Psi_3 = 0 \quad (SBA, X > 0, Y = H(X)), \tag{22}$$

$$N_3 = -U_1 U_3 - \tfrac{1}{2}U_2^2 - \tfrac{1}{2}U_1(U_1 N_{1,x}^2 - 2N_1 V_{2,x} - N_1^2 U_{1,xx}) \quad (X < 0, Y = 0), \tag{23}$$

where $H = h'/T'$, $h'(x')$ being a function defining the body shape.

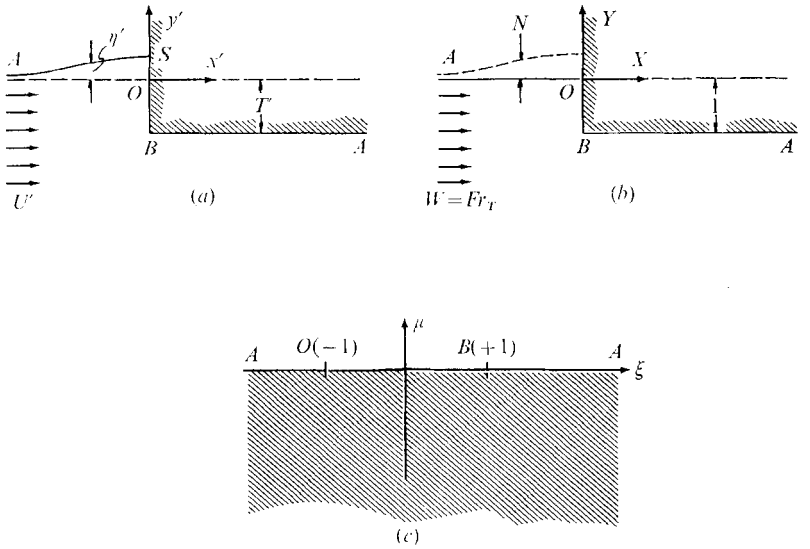

FIGURE 3. Small Fr_T flow past a box-like body. (*a*) The physical plane, $z' = x' + iy'$; (*b*) the linearized dimensionless physical variables, $Z = X + iY$; (*c*) the auxiliary ζ plane, $\zeta = \xi + i\mu$.

At second and third order the flow is generated by source distributions along the degenerate free surface (equations (18) and (21)). It is easy to ascertain that both Ψ_2 and Ψ_3 are zero at infinity and at the origin, such that the total source flux is zero. The drag is also zero at any order.

2.3. *Solution for a rectangular body*

For the sake of simplicity we have solved the equations, to second order, for the box-like body of figure 3(*a*). The solution of the first-order approximation is obtained in terms of the auxiliary variable ζ as

$$W_1 = [(\zeta + 1)/(\zeta - 1)]^{\frac{1}{2}}, \quad F_1 = \zeta/\pi, \tag{24}$$

where the mapping of the linearized Z plane (figure 3(*b*)) onto the ζ plane (figure 3(*c*)) is given by

$$Z = (1/\pi)(\zeta^2 - 1)^{\frac{1}{2}} + (1/\pi)\ln[(\zeta^2 - 1)^{\frac{1}{2}} - \zeta]. \tag{25}$$

Hence, from (17) we have

$$N_1 = 1/(1 - \xi) \quad (\xi < -1). \tag{26}$$

For the second-order approximation (equation (18)) we get

$$\Psi_2 = (\xi + 1)^{\frac{1}{2}}/(\xi - 1)^{\frac{3}{2}} \quad (\xi < -1, \mu = 0). \tag{27}$$

If Ψ_2 is given along the real ζ axis (equations (19) and (29)) then by Cauchy integration

$$\Phi_2(\xi) = -\frac{1}{\pi}\mathrm{Re}\int_{-1}^{-\infty}\Psi_2(\lambda)\frac{d\lambda}{\xi-\lambda} = -\frac{1}{\pi}\left\{\frac{2}{1-\xi}+\left(\frac{\xi+1}{\xi-1}\right)^{\frac{1}{2}}\frac{\ln\left[-\xi-(\xi^2-1)^{\frac{1}{2}}\right]}{1-\xi}\right\}. \quad (28)$$

U_2 and N_2 as functions of ξ are easily found from (20) and (28) (for details see Dagan & Tulin 1969). The shape of the free surface at second order is given in figure 4. The first-order solution (17) gives the exact values of N at infinity and at the stagnation point. A detailed check shows that not only N_2 (equation (20)) but also N_3 (equation (23)) vanish at these two anchor points, the higher order approximations correcting only the shape of the free surface in the intermediate range. The small Fr_T expansion (12)–(14) is consistent and seems to be uniformly convergent (at least at third order). It differs from that suggested by Ogilvie (1968) who obtained waves far behind a submerged body. Figure 4 shows that the free-surface profile becomes steep as Fr_T increases. We can expect, therefore, that at a certain critical Fr_T it will become unstable.

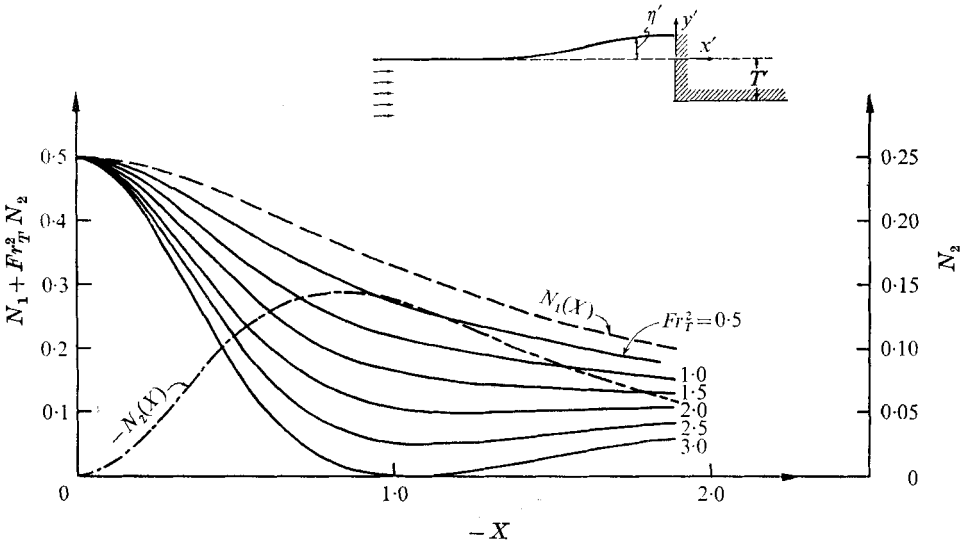

FIGURE 4. The free-surface shape in front of a rectangular body, with $N(X)$ as in (14).

2.4. *The stability of the free surface*

According to the Taylor local criterion (see § 1) the free surface becomes unstable at the point where the normal pressure gradient vanishes, i.e. for

$$\partial p'/\partial n' = -\rho g(1+\eta'^2_{,x'})^{-\frac{1}{2}}+\rho(u'^2+v'^2)/r' = 0 \quad (29)$$

or, in dimensionless variables,

$$\partial p/\partial n = -(U^2+V^2)N_{,XX}(1+N_{,X})^{-\frac{3}{2}}-(1+N^2_{,X})^{-\frac{1}{2}} = 0. \quad (30)$$

The pressure vanishes in the region of convexity of the free surface ($N_{,XX} < 0$). By the expansion of (30) along $Y = N(X)$ the stability condition becomes

$$-1+Fr_T^4\left[\frac{1}{2}\left(\frac{dN_1}{dX}\right)^2-U_1^2\frac{d^2N_1}{dX^2}\right]+Fr_T^6\left(\frac{dN_1}{dX}-U_1^2\frac{d^2N_2}{dX^2}-2U_1U_2\frac{d^2N_1}{dX^2}\right) = 0, \quad (31)$$

where only the first two terms of the expansion contribute up to the order Fr_T^6 in the pressure gradient expression. Taylor's marginal stability is reached for the value of Fr_T which satisfies (31) equal to zero. This value has been found to be $Fr_T \simeq 1{\cdot}5$ and the point of instability is at $X = 0{\cdot}3$.

Although the expression for the pressure gradient can hardly be expected to converge rapidly at such a high Fr_T, the result is of the order of magnitude of that found by Baba (1969) and would seem to confirm the mechanism of free-surface disruption assumed here. The effect is nonlinear since only when the second-order term is taken into account does the steepening of the free surface depend strongly on Fr_T. There is no bow drag in the small Fr_T limit. The present method suggests a possible way of determining the influence of the bow shape on the breaking wave inception and therefore serves to select shapes which retard the phenomenon.

3. The high Froude number solution

3.1. *The exact equations*

In this case we adopt the jet model (figures 1(*c*) and 5(*a*)) for the representation of the bow momentum loss. The returning jet is neglected, since the jet thickness turns out to be a second-order quantity. Using a procedure followed in similar problems in the past (Tulin 1965; Wu 1967) we map the flow domain onto the complex potential plane $f = \phi + i\psi$ (figure 5(*b*)). The variables are outer variables and are made dimensionless by referring them to U' and U'^2/g. For convenience we map f on the auxiliary half ζ plane (figure 5(*c*)) by the transformation

$$df/d\zeta = 1 - t/\pi\zeta \tag{32}$$

where t is the dimensionless jet thickness (actual jet thickness $t' = tU'^2/g$).

The exact boundary conditions for the complex velocity w ($w = w'/U'$), given here for convenience of reference, are as follows

$$\mathrm{Re}\left\{\overline{w}^2 w \frac{dw/d\zeta}{1 - t/\pi\zeta} + iw\right\} = 0 \quad (AJ), \tag{33}$$

$$\arg w = -\arctg dh/dx \quad (SJ), \tag{34}$$

$$\arg w = \arctg dh/dx \quad (SBA), \tag{35}$$

$$w \to 1 \quad (\zeta \to -\infty), \tag{36}$$

where $y = h(x)$ is the profile equation ($h = h'g/U'^2$). The physical plane is mapped on the ζ plane by

$$z = \int_{-\infty}^{\zeta} \frac{1 - t/\pi\zeta}{w} d\zeta. \tag{37}$$

3.2. *Outer expansion*

We consider now a perturbation expansion near the state of uniform flow with $\epsilon = 1/Fr_T^2$ as a small parameter. By definition $h(x) = \epsilon h_1(x)$. We also assume that $t = o(1)$ and we anticipate a later result by estimating $t = O(\epsilon^2)$. Hence, for the

outer observer the body shrinks to the line $y = 0$ and the points S, O, J (figure 5(c)) collapse into the origin of the ζ plane when $\epsilon \to 0$. With

$$w = 1 + \delta_1(\epsilon)\, w_1(\zeta) + \delta_2(\epsilon)\, w_2(\zeta) + \ldots \tag{38}$$

we have at zero order

$$z = \zeta, \tag{39}$$

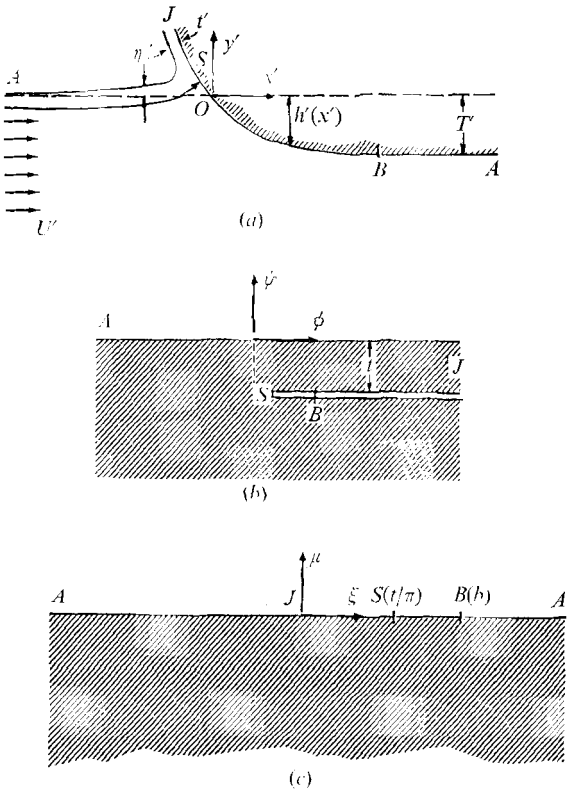

FIGURE 5. Free-surface flow past a semi-infinite body (high Fr_T). (*a*) The physical plane, $z' = x' + iy'$ ($z' = zU'^2/g$); (*b*) the complex potential plane, $f = \phi + i\psi$; (*c*) the auxiliary ζ plane, $\zeta = \xi + i\mu$.

while at first order we obtain from (33)–(37)

$$\mathrm{Re}\,(dw_1/d\zeta + iw_1) = 0 \quad (\xi < 0,\ \mu = 0), \tag{40}$$

$$w_1 = 0 \quad (\xi \to -\infty), \tag{41}$$

$$z = \zeta - \epsilon \int_{-\infty}^{\zeta} w_1\, d\zeta, \tag{42}$$

where $\delta_1 = \epsilon$, as a result of (35).

Along the body ($\xi > 0$, $\mu = 0$) equation (42) gives

$$x = \xi, \quad h_1(x) = -\mathrm{Im} \int_{-\infty}^{\xi} w_1\, d\zeta. \tag{43}$$

Hence, with $k_1(\zeta) = \int_{-\infty}^{\zeta} w_1 d\zeta$ we finally obtain from the integration of (40)

$$\mathrm{Re}\,(w_1 + ik_1) = 0 \quad (\xi < 0, \mu = 0), \tag{44}$$

$$\mathrm{Im}\,k_1(\zeta) = -h_1(\xi) \quad (\xi > 0, \mu = 0). \tag{45}$$

Equations (44) and (45) permit the computation of w_1, which in turn yields z from (42).

By similar reasoning we arrive at the following equations for the second order:

$$\mathrm{Re}\,(dw_2/d\zeta + iw_2) = -\mathrm{Re}\,[(w_1 + 2\overline{w}_1)\,dw_1/d\zeta] \quad (\xi < 0, \mu = 0), \tag{46}$$

$$\mathrm{Im}\,w_2 = -\tfrac{1}{2}\,\mathrm{Im}\,w_1^2 \quad (\xi > 0, \mu = 0), \tag{47}$$

$$w_2(\zeta) \to 0 \quad (\xi \to -\infty), \tag{48}$$

where $\delta_2 = \epsilon^2$.

To solve at first order we adopt a procedure similar to that followed in planing problems (Squire 1957), i.e. we replace the body by an unknown pressure distribution $g_1(\xi)$ along $\mu = 0$, $\xi > 0$ and determine g_1 such that (44) and (45) are satisfied.

The flow due to a pressure force of unit strength acting on the free surface at $\xi = \nu$ is represented by the linearized potential (Stoker 1957)

$$m(\zeta) = \frac{i}{\pi} e^{-i(\zeta-\nu)} E[i(\zeta-\nu)], \tag{49}$$

where

$$E(i\zeta) = \int_{-\infty}^{\zeta} \frac{e^{iu}}{u}\,du \tag{50}$$

and the integration in (50) is carried out along a path entirely lying in the lower half u plane. The singularity of m near $\zeta = \nu$ is of a vortex type, so that in fact we have replaced the body by a vortex distribution.

The function $k_1(\zeta)$ has, therefore, the expression

$$k_1(\zeta) = \frac{1}{\pi}\int_0^{\infty} e^{-i(\zeta-\nu)} E[i(\zeta-\nu)]\, g_1(\nu)\,d\nu \tag{51}$$

and satisfies (44). Equation (45) now becomes, with the aid of (51),

$$\frac{1}{\pi}\int_0^{\infty} \mathrm{Re}\{e^{-i(\xi-\nu)} E[i(\xi-\nu)]\}\, g_1(\nu)\,d\nu = -h_1(\xi) \quad (\xi > 0). \tag{52}$$

The solution of this integral equation gives $g_1(\xi)$, which in turn permits the determination of $k_1(\zeta)$ and $w_1(\zeta) = dk_1/d\zeta$. Equation (52), with a displacement kernel, may be solved by the Wiener–Hopf technique. In fact, an almost identical equation has been studied by Carrier, Krook & Pearson (1966, p. 397). By applying the integral Fourier transform to (52) we obtain

$$M(\lambda)\, G_1^+(\lambda) = \frac{1}{(2\pi)^{\frac{1}{2}}}[N_1^-(\lambda) + H^+(\lambda)]. \tag{53}$$

In the appendix we prove that

$$M(\lambda) = \frac{1}{(2\pi)^{\frac{1}{2}}}\int_{-\infty}^{\infty} e^{i\lambda\nu}\,[\mathrm{Re}\,(e^{-i\nu} E(i\nu))]\,d\nu = \frac{1}{(2\pi)^{\frac{1}{2}}}\frac{1}{(1+|\lambda|)} \tag{54}$$

and since this is exactly the transform of the kernel considered by Carrier *et. al* (1966, p. 396) we at once adopt their factorization

$$M^{+}(\lambda) = \frac{1}{(1+\lambda)^{\frac{1}{2}}} \exp\left[\frac{1}{\pi i}\int_0^{\lambda} \frac{\ln u}{1-u^2}\,du\right], \tag{55}$$

$$M^{-}(\lambda) = \frac{1}{(2\pi)^{\frac{1}{2}}}\frac{1}{(1+\lambda)^{\frac{1}{2}}} \exp\left[-\frac{1}{\pi i}\int_0^{\lambda} \frac{\ln u}{1-u^2}\,du\right]. \tag{56}$$

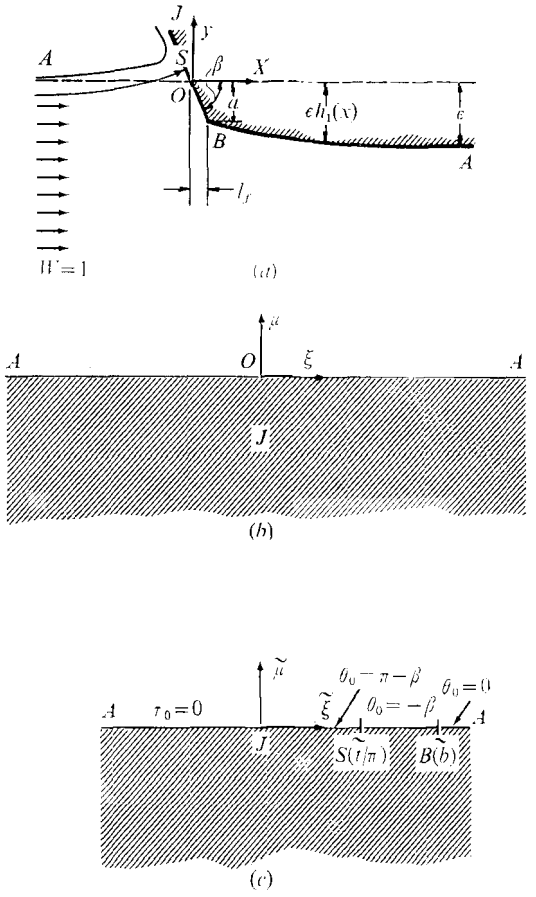

FIGURE 6. Two-dimensional flow past a blunt body (high Fr_T). (*a*) The physical plane; (*b*) the body boundary condition in the outer approximation with

$$h_1(x) = -a + (1-a)\,(e^{-x/l} - 1) \quad \text{for} \quad \mu = 0,\ \xi = 0;$$

(c) the body boundary condition in the zeroth-order inner approximation, $\tilde{\zeta} = \tilde{\xi} + i\tilde{\mu}$, symbols with a tilde as defined in (67).

The separation of (53) may be now accomplished provided that we select a given body shape, i.e. the function $h_1(x)$. We limit ourselves here to the case of a blunt body (figure 6 (*a*)), with $h_1(x)$ as follows:

$$h_1(x) = -a\,x/l_f \quad (0 < x < l_f), \tag{57}$$

$$h_1(x) = -a + (1-a)\,[e^{-(x-l_f)/l} - 1] \quad (x > l_f), \tag{58}$$

where a is the (dimensionless) draft at the bow of a completely blunt shape, $0 < a < 1$; $l = l'g/U'$, $l_f = l_f g/U'$ (l' and l'_f being the characteristic and forebody lengths respectively) and $l = O(1)$. The dimensionless forebody length l_f is assumed to be of order ϵ, so that in the limit process $\epsilon \to 0$ the angle β (the angle at the bow) is kept fixed. Under these conditions, in the outer limit the body degenerates at first order in a box-like body, with equation

$$h_1(x) = -a + (1-a)(e^{-x/l} - 1) \quad (x > 0). \tag{59}$$

The shape of figure 6 has been selected for the sake of simplicity. Any shape with a forebody of order ϵ (completely blunt) and $l = O(1)$ yields the same solution in the vicinity of the bow. When $a = 0$ the bluntness disappears and the shape is fine, while for $a = 1$ the aftbody is flat.

From (59) we obtain

$$H^+(\lambda) = -\frac{1}{(2\pi)^{\frac{1}{2}}}\int_0^\infty e^{i\lambda\nu} h_1(\nu)\, d\nu = -\frac{1}{(2\pi)^{\frac{1}{2}}}\frac{1}{i\lambda} + \frac{1-a}{(2\pi)^{\frac{1}{2}}}\frac{1}{(i\lambda - 1/l)} \tag{60}$$

and from the separation of (53)

$$G_1^+(\lambda) = \frac{i}{2\pi}\left[\frac{1}{\lambda} - (1-a)\frac{1}{\lambda + i/l}\right]\frac{1}{M^+(\lambda)}\frac{1}{M^-(0)} + \left\{\sum_{i=0}^{n} c_{1i}\lambda^i\right\} \Big/ M^+(\lambda), \tag{61}$$

where the last term, representing eigensolutions, results from the application of Liouville's theorem, c_{1i} being arbitrary.

Equation (61) cannot be inverted exactly, because of the integral appearing in $M^+(\lambda)$, but the inversion can be carried out for large λ by expanding $M^+(\lambda)$. After carrying out this process (see Dagan & Tulin 1970) we arrive at the following expression for $g_1(\xi)$ in the vicinity of the origin:

$$g_1(\xi) = \frac{a}{(\pi\xi)^{\frac{1}{2}}} + O(\xi^{\frac{1}{2}} \ln \xi) + \sum_{i=0}^{n} \frac{d_{1i}}{\xi^{i+\frac{1}{2}}} \quad (\xi \to 0), \tag{62}$$

where the d_{1i} are constants related in a unique manner to c_{1i}. From (62) we obtain

$$w_1(\zeta) = -\frac{a}{(\pi\zeta)^{\frac{1}{2}}} + O(\zeta^{\frac{1}{2}} \ln \zeta) + \sum_{i=0}^{n} \frac{d_i}{\zeta^{i+\frac{1}{2}}} \quad (\zeta \to 0), \tag{63}$$

which is the central result of our analysis.

The expression of the second-order solution, satisfying (22), (23) and (32), was found to be

$$w_2(\zeta) = \frac{a^2}{2\pi\zeta} + O(\ln \zeta) + \sum_{i=0}^{n} \frac{d_{1i}}{\zeta^{i+\frac{1}{2}}} \quad (\zeta \to 0). \tag{64}$$

Summarizing the results obtained so far, we have

$$w = 1 - \frac{\epsilon a}{(\pi\zeta)^{\frac{1}{2}}} + \frac{\epsilon^2 a^2}{2\pi\zeta} + \epsilon O((\zeta)^{\frac{1}{2}} \ln \zeta) \quad (\zeta \to 0), \tag{65}$$

$$\frac{dz}{d\zeta} = 1 - \delta_1 w_1 - \delta_2(w_2 - w_1^2) - \frac{t}{\pi\zeta} + \ldots = 1 + \frac{\epsilon a}{(\pi\zeta)^{\frac{1}{2}}} + \frac{\epsilon^2}{2\pi}\frac{1}{\zeta} - \frac{t}{\pi\zeta} + \ldots, \tag{66}$$

where the eigensolutions have been omitted because they yield infinite forces.

The velocity has the familiar square-root singularity at first order and a source singularity at second order. The free surface is continuous at first order, while at second order it rises at infinity. The eigensolutions of the problem, which represent in fact the linearized solutions of a free-surface flow past a flat horizontal plate, as well as the flow details near the bow will be subsequently determined with the aid of an inner solution. It is worth while to mention here that only at second order are the details of the adopted model (i.e. the jet) manifested in the solution. Any other flow model will produce an identical first-order solution.

3.3. *The inner expansion and its matching with the outer solution*

We now stretch the co-ordinates and adopt the following inner variables:

$$\tilde{\zeta} = \zeta/\epsilon, \quad \tilde{w} = w, \quad \tilde{z} = z/\epsilon, \quad \tilde{t} = t/\epsilon, \quad \tilde{b} = b/\epsilon, \tag{67}$$

where b is the outer co-ordinate of a point B in the ζ plane, and expand the function $\tilde{\Omega} = \ln(1/\tilde{w}) = \tau + i\theta$ in a perturbation series

$$\tilde{\Omega} = \tilde{\Omega}_0 + \Delta_1(\epsilon)\,\tilde{\Omega}_1 + \dots . \tag{68}$$

For the body of figure 6(*a*) we obtain from the inner expansion of the exact equations the boundary conditions for $\tilde{\Omega}_0$ specified in figure 6(*c*) which represent a nonlinear free-surface flow without gravity (for details see Dagan & Tulin 1970). The conditions at infinity are provided by matching with the outer expansion. Only in the case of the straight bow of figure 6(*a*) are the inner conditions so simple. In the general case we have to solve an integral equation for θ (Wu 1967) or start with a given $\theta(\tilde{\xi})$.

The solution of $\tilde{w}_0$ is readily found in the form

$$w_0 = \frac{\tilde{\zeta}^{\frac{1}{2}} - (\tilde{t}/\pi)^{\frac{1}{2}}}{\tilde{\zeta}^{\frac{1}{2}} + (\tilde{t}/\pi)^{\frac{1}{2}}} \left[\frac{\tilde{\zeta}^{\frac{1}{2}} + \tilde{b}}{\tilde{\zeta}^{\frac{1}{2}} - \tilde{b}}\right]^{\beta/\pi} \exp\left(\sum_i \frac{\tilde{d}_{0i}}{\tilde{\zeta}^{i+\frac{1}{2}}}\right), \tag{69}$$

where the exponential represents the eigensolutions of the problem, the $\tilde{d}_{0i}$ being arbitrary constants. Expanding $\tilde{w}_0$ for large $\tilde{\zeta}$ we obtain

$$\tilde{w}_0 = 1 - 2\left[\left(\frac{\tilde{t}}{\pi}\right)^{\frac{1}{2}} - \frac{\beta\tilde{b}^{\frac{1}{2}}}{\pi}\right]\frac{1}{\tilde{\zeta}^{\frac{1}{2}}} + 2\left[\left(\frac{\tilde{t}}{\pi}\right)^{\frac{1}{2}} - \frac{\beta\tilde{b}^{\frac{1}{2}}}{\pi}\right]^2 \frac{1}{\tilde{\zeta}} + \frac{\tilde{d}_{04}}{\tilde{\zeta}^{\frac{1}{2}}} + \dots . \tag{70}$$

According to our estimate $\tilde{t} = O(\epsilon)$ and $\tilde{b} = O(1)$. To match $\tilde{w}_0$ in (10) with w in (65) we have therefore to assume that the term in $\tilde{b}^{\frac{1}{2}}$ in (70) has to be absorbed by the eigensolution or has to generate in the outer solution a new term of order $\epsilon^{\frac{1}{2}}$. In any case the matching requires

$$\tilde{t} = \tfrac{1}{4}\epsilon a^2, \quad \text{i.e.} \quad t = \tfrac{1}{4}\epsilon^2 a^2. \tag{71}$$

The bow drag associated with the momentum loss in the jet is therefore

$$\tilde{D} = \tfrac{1}{4}\epsilon^2 a^2 (1 + \cos\beta), \tag{72}$$

where $D = D'/\rho U'^2 T'$ and D' is the drag.

To roughly compare the result of (72) with Baba's findings, we assume that the bow in his experiments is completely blunt with $\beta = \frac{1}{2}\pi$ and $a = 1$. For $\epsilon = 1/Fr_T^2 \approx 0{\cdot}34$ we have

$$C_D = 2\tilde{D} = 0{\cdot}17, \tag{73}$$

which is roughly twice as large as the value estimated by Baba. At this stage it is difficult to find which of the following factors explain this discrepancy: the asymptotic character of the solution, the lack of details on the bow shape or the crude representation by Baba of a three-dimensional flow by a two-dimensional equivalent. Future experiments and theoretical developments will give the answer to this question.

The method presented here is applicable to other bow shapes, like blunt round bows. In this latter case the bow drag appears at higher order than in the completely blunt case. The extension to other shapes, as well as to three-dimensional bodies, is left for future studies.

4. Conclusions

Theoretical models of breaking wave inception and of a free-surface bow drag have been derived for the case of a two-dimensional free-surface gravity flow past a blunt body. In both cases the effects are nonlinear and are related to the important role played by the inertial term of the Bernoulli equation in the vicinity of the bow. The results lead to a drag force about twice as large as that estimated by Baba (1969), but an improved verification has to be done by carrying out two-dimensional experiments.

The present work has been supported by O.N.R. through contract Nonr-3349(0)0 Nr 062-266 with Hydronautics, Inc.

Appendix. The Fourier transform of the kernel of equation (52)

The kernel has the following expression:

$$m(\xi) = \frac{1}{\pi}\mathrm{Re}\,[e^{i\xi}\,E(i\xi)], \tag{A 1}$$

where $E(i\xi)$ is defined by (50). With $u = \xi + is$ the kernel becomes

$$m(\xi) = \frac{1}{\pi}\mathrm{Re}\left\{e^{i\xi}\int_{-\infty}^{\xi}\frac{e^{iu}}{u}du\right\} = \frac{1}{\pi}\mathrm{Re}\int_{i\infty}^{0}\frac{e^{-s}}{s-i\xi}ds, \tag{A 2}$$

the integration contour being transferred from the lower half plane to the imaginary axis of the s plane, leaving the pole $s = i\xi$ on the right. By closing the integration contour in the first quadrant we obtain

$$\int_{i\infty}^{0}\frac{e^{-s}}{s-i\xi}ds = 2\pi i - \int_{0}^{\infty}\frac{e^{-s}}{s-i\xi}ds \quad \text{for} \quad \xi > 0 \tag{A 3}$$

and

$$\int_{i\infty}^{0}\frac{e^{-s}}{s-i\xi}ds = -\int_{0}^{\infty}\frac{e^{-s}}{s-i\xi}ds \qquad \text{for} \quad \xi < 0. \tag{A 4}$$

Hence in both cases

$$m(\xi) = \frac{1}{\pi}\mathrm{Re}\,[e^{-i\xi}E(i\xi)] = -\frac{1}{\pi}\mathrm{Re}\int_0^\infty \frac{e^{-s}}{s-i\xi}ds = -\frac{1}{\pi}\int_0^\infty \frac{s\,e^{-s}}{s^2+\xi^2}ds. \qquad \text{(A 5)}$$

The Fourier transform of $m(\xi)$ is given by

$$M(\lambda) = -\frac{1}{\pi(2\pi)^{\frac{1}{2}}}\int_0^\infty \int_{-\infty}^\infty \frac{s\,e^{i\lambda\xi-s}}{s^2+\xi^2}d\xi\,ds,$$

which by the residue theorem gives

$$M(\lambda) = -\frac{1}{(2\pi)^{\frac{1}{2}}}\int_0^\infty e^{-s-|\lambda|s}ds = \frac{1}{(2\pi)^{\frac{1}{2}}}\frac{1}{(1+|\lambda|)}. \qquad \text{(A 6)}$$

REFERENCES

BABA, E. 1969 Study on separation of ship resistance components. *Mitsubishi Tech. Bull.* no. 59, p. 16.

CARRIER, G. F., KROOK, M. & PEARSON, C. E. 1966 *Functions of a Complex Variable.* McGraw-Hill.

DAGAN, G. & TULIN, M. P. 1969 Bow waves before blunt ships. *Hydronautics. Inc. Tech. Rep.* pp. 117–14.

DAGAN, G. & TULIN, M. P. 1970 The free-surface bow drag of a two-dimensional blunt body. *Hydronautics Inc. Tech. Rep.* pp. 117–17.

EGGERS, K. W. H. 1966 On second-order contributions to ship waves and wave resistance. *Proc. 6th Symp. of Naval Hydrodynamics.*

OGILVIE, T. F. 1968 Wave resistance: the low-speed limit. *Dept. of Naval Arch., Univ. of Michigan. Rep.* no. 002, p. 29.

SQUIRE, H. B. 1957 The motion of a simple wedge along the water surface. *Proc. Roy. Soc.* A **243**, 48–64.

STOKER, J. J. 1957 *Water Waves.* Wiley.

TAYLOR, G. I. 1950 The instability of liquid surfaces when accelerated in a direction perpendicular to their plane. Part I. *Proc. Roy. Soc.* A **201**, 192.

TUCK, E. O. 1965 A systematic asymptotic procedure for slender ships. *J. Ship Res.* **8** (1), 15–23.

TULIN, M. P. 1965 Supercavitating flows – small perturbation theory. *Proc. IUTAM, Symp. on the Application of the Theory of Functions in Continuous Mechanics,* **2**, 403–439.

VAN DYKE, M. 1964 *Pertubation Methods in Fluid Mechanics.* Academic.

WEHAUSEN, J. V. & LAITONE, E. V. 1960 Surface waves. In *Encyclopedia of Physics,* vol. IX, pp. 446–779. Springer.

WEINBLUM, G. P., KENDRIK, J. J. & TODD, M. A. 1952 Investigation of wave effects produced by a thin body. *David Taylor Model Basin Rep.* no. 840, p. 19.

WU, T. Y. 1967 A singular perturbation theory for nonlinear free-surface flow problems. *Int. Shipbldg Prog.* **14**, (151), 88–97.